



Antigenicity modulation upon peptide cyclization: application to the GH loop of foot-and-mouth disease virus strain C₁-Barcelona[☆]

Paula Gomes¹, Ernest Giralt, David Andreu^{*}

Department of Organic Chemistry, University of Barcelona, Martí i Franquès 1, E-08028 Barcelona, Spain

Received 1 November 2000; received in revised form 22 January 2001; accepted 30 January 2001

Abstract

Foot-and-mouth disease virus (FMDV) isolate C₁-Barcelona (or C-S30) includes four replacements within its immunodominant site (GH loop, residues 136–150 of capsid protein VP1, YTTSTRGDLAHVTTAT), relative to reference strain C-S8c1 (YTASARGDLAHLTTT). Although one of the mutations in C-S30 (¹⁴⁷Leu → Val) is known to be detrimental for antibody recognition, reactivity of this isolate with the neutralizing monoclonal antibody (mAb) 4C4, raised against FMDV C₁-Brescia (GH loop: YTASTRGDLAHLTAT), was indistinguishable from those of strains C-S8c1 or C₁-Brescia. A structural interpretation for these somewhat striking findings is available, based on the observation that 15-residue peptides reproducing the C-S30 and C-S8c1 GH loops adopt very similar, quasi-circular, conformations in crystal complexes with 4C4. Nevertheless, surface plasmon resonance (SPR) kinetic analyses of the interactions between these peptides and three anti-GH loop mAbs have now revealed that the linear C-S30 peptides were less antigenic in solution than their C-S8c1 and C₁-Brescia counterparts. We have, therefore, tried to modulate peptide antigenicity in solution by cyclization. Functional SPR and structural two dimensional proton nuclear magnetic resonance (2D-¹H NMR) studies of both linear and cyclic peptide antigens are discussed here. Conformation seems to have an important role in peptide antigenicity, even when continuous (i.e. linear) antigenic sites are involved. © 2001 Elsevier Science Ltd. All rights reserved.

Keywords: Antibody-antigen recognition; BIAcore; Foot-and-mouth disease virus; Surface plasmon resonance; Peptide conformation

1. Introduction

Foot-and-mouth disease virus (FMDV), an aphthovirus from the *Picornaviridae* family, causes the

economically most important disease of farm animals [1] and is characterized by an extremely high antigenic and genetic variability that gives rise to seven serotypes and over 65 subtypes. In serotype C, neutralizing anti-

Abbreviations: 2D-¹H NMR, two-dimensional proton nuclear magnetic resonance; AA, amino acid residue; AAA, amino acid analysis; Ahx, 6-aminohexanoic acid; AM, 2-[4-aminomethyl-(2,4-dimethoxyphenyl)]phenoxyacetic acid (linker); C_A, analyte concentration; ΔδH_α, conformational chemical shift for proton α; DIEA, diisopropylethylamine; DMF, *N,N'*-dimethylformamide; EDC, *N*-ethyl-*N'*-dimethylaminopropylcarbodiimide; EID, enzyme immunodot; EITB, enzyme immuno-electrotransfer blot; ESIMS, electrospray ionization mass spectrometry; Et₃Si, triethylsilane; Fab, fragment antigen binding; FMDV, foot-and-mouth disease virus; Fmoc, 9-fluorenylmethoxycarbonyl; HPLC, high performance liquid chromatography; IC₅₀, 50% inhibition concentration; k_a, association rate constant (M⁻¹s⁻¹); K_A, association thermodynamic constant (M⁻¹); k_d, dissociation rate constant (s⁻¹); K_D, dissociation thermodynamic constant (M); KLH, keyhole limpet hemocyanin; K_f, solution affinity constant (M⁻¹); mAb, monoclonal antibody; MALDI-TOF MS, matrix-assisted laser desorption — time-of-flight mass spectrometry; MBHA, *p*-methylbenzhydrylamine resin; MeCN, acetonitrile; NHS, *N*-hydroxysuccinimide; NMM, *N*-methylmorpholine; NOE, nuclear Overhauser effect; PBS, phosphate buffer saline; R_{eq}, equilibrium response; RI, bulk refractive index; R_{immob}, immobilization response; R_{max}, maximum response (RU); RPLC, reverse phase liquid chromatography; RU, resonance units; SPSS, solid phase peptide synthesis; SPR, surface plasmon resonance; ^tBu, *tert*-butyl; TBTU, 2-(1H-benzotriazole-1-yl)-1,1,3,3-tetramethyluronium tetrafluoroborate; TFA, trifluoroacetic acid; TFE, 2,2,2-trifluoroethanol.

[☆] Part of this work was presented as a poster communication at the 26th European Peptide Symposium, Montpellier (France), September 2000.

^{*} Corresponding author. Tel./fax: +34-93-4021260.

E-mail address: andreu@qo.ub.es (D. Andreu).

¹ Present address: C. I. Q. — “Centro de Investigação em Química”, Department of Chemistry, University of Porto, P-4169-007 Porto, Portugal.

Table 1
Synthetic peptide mimics of the GH loops from serotype C FMD viruses

Peptide	Sequence	Comments
A15S8c1	YTASARGDLAHLTTT	GH loop of FMDV C-S8c1
A15Brescia	----T-----A-	GH loop of FMDV C ₁ -Brescia
A15S30	--T-T-----V-A-	GH loop of FMDV C-S30
cycl16S30 ^{a,b}	(C--T-T-----V-AXC)	GH loop of FMDV C-S30 (cyclic)

^a X stands for a 6-aminohexanoic acid residue.

^b Parenthesis stand for an intra-molecular Cys–Cys bond (cyclic peptide).

bodies recognize FMDV GH loop (residues 136–150 of capsid protein VP1 [2]), which includes several overlapping linear epitopes [3] and is also termed antigenic site A. Site A includes highly conserved residues, such as an Arg–Gly–Asp (RGD) motif, and two leucines (¹⁴⁴Leu, ¹⁴⁷Leu), which are deeply involved in cell and antibody recognition events [4]. This immunodominant region can be faithfully reproduced by synthetic linear peptides with the sequences found in the different virus isolates [5–7]. Thus, the GH loop of FMDV C₁-Santa Pau Sp/70 (C-S8c1) is reproduced by peptide A15S8c1 (YTASARGDLAHLTTT, Table 1). The interactions of this peptide with neutralizing monoclonal antibodies (mAb), such as SD6 (raised against C-S8c1), 4C4 or 3E5 (both raised against C₁-Brescia), have been fully characterized by means of enzyme-linked immunosorbent assays (ELISA), surface plasmon resonance (SPR) biosensor analysis and X-ray crystallographic studies [8–11]. This peptide displayed high reactivity with both mAbs and acquired a quasi-circular conformation when in crystal complexes with both fragment antigen binding (Fab) fragments of SD6 and 4C4.

Recent crystallographic studies showed that another peptide representing the GH loop of the variant isolate C-S30 (peptide A15S30, YTTSTRGDLAHVTAT) also adopts this quasi-circular conformation in the crystal complex with Fab 4C4 [12]. Earlier immuno-enzymatic studies had also shown that keyhole limpet hemocyanin (KLH) conjugates of 21-mer peptides reproducing the GH loops of C-S30, C-S8c1 and C₁-Brescia strains [13] were all recognized by mAb 4C4 to a similar extent. Relative to strain C-S8c1, FMDV C-S30 includes four mutations within the GH loop, two of them also present in FMDV C₁-Brescia (¹⁴⁰Ala → Thr, ¹⁴⁹Thr → Ala). The fact that one of these mutations, ¹⁴⁷Leu → Val, is known to be detrimental for antibody and cell recognition, makes the C-S30 peptides interesting targets in the study of antigen–antibody recognition mechanisms.

In this work, we have functionally characterized the antibody recognition patterns of FMDV strain C-S30 by SPR analysis of representative synthetic peptides. While SPR binding data on peptide A15S30 (YTTSTRGDLAHVTAT) and mAb SD6 were totally self-consistent, its reactivity towards 4C4 was surprisingly lower

than those of peptides A15S8c1 (YTASARGDLAHLTTT) or A15Brescia (YTASTRGDLAHLTAT). In view of these unexpected results, we studied the A15S30 — mAb interaction in solution by means of a solution affinity SPR experiment. Finally, as done earlier for a C-S8c1-derived peptide [14], we have introduced conformational restrictions in the C-S30 loop, by means of an intramolecular disulfide bridge. The resulting cyclic peptide reproduces to a good extent the SPR binding behavior expected from earlier data, and its structural analysis by 2D-¹H NMR is consistent with the adoption of a native-like conformation.

2. Materials and methods

2.1. Peptides

Linear peptides A15S8c1, A15Brescia, A15S30 and the dithiol precursor of cycl16S30 (Table 1) were synthesized by SPPS as C-terminal carboxamides on an AM-MBHA resin (0.51 mmol g⁻¹) using 9-fluorenylmethoxycarbonyl/*tert*-butyl (Fmoc/*t*Bu) chemistry [15,16]. The synthesis scale was 0.1 mmol and couplings were done with 4, 4 and 8 equivalents of Fmoc-amino acid residue (AA)-OH, 2-(1H-benzotriazole-1-yl)-1,1,3,3-tetramethyluronium tetrafluoroborate (TBTU) and diisopropylethylamine (DIEA), respectively. A 20% piperidine solution in *N,N'*-dimethylformamide (DMF) was used for the Fmoc deprotection steps. Peptides were fully deprotected and cleaved from the resin with trifluoroacetic acid/triethylsilane/H₂O (TFA/Et₃Si/H₂O) (95:2.5:2.5 v/v) for 2 h. The peptides were isolated from the cleavage solution by precipitation with cold *t*Bu methyl ether, solubilized in diluted HOAc, lyophilized and purified by reverse phase liquid chromatography (RPLC) using a linear 5 → 25% gradient of acetonitrile (MeCN) into 0.05% TFA in water. Purified products were satisfactorily characterized by amino acid analysis (AAA), high performance liquid chromatography (HPLC) and electrospray ionization mass spectrometry (ESIMS). Cyclization of cycl16S30 was done by air oxidation of the free thiol groups at 50 μM peptide in 100 mM NH₄HCO₃, pH 8. The reaction was stopped by addition of glacial acetic acid after 2 h.

After several lyophilization steps the cyclic disulfide peptide was isolated and characterized as above.

Stock solutions (ca. 2.5 mM) of the above peptides in 0.1 M acetic acid were prepared and quantitated by AAA. For SPR analysis, 1000-fold and subsequent serial dilutions in HBS of the stock solutions were used.

2.2. Monoclonals and Fab fragments

Monoclonals SD6 and 4C4 and their Fab fragments were a gift from Drs Wendy Ochoa and Nuria Verdager, IBMC/CSIC, Barcelona, Spain. Stock solutions in phosphate buffer saline (PBS) with 0.02% sodium azide, pH 7.3 were quantitated by the Pierce BCA assay (Pierce & Co.). Solutions for mAb immobilization (in 10 mM acetate buffer, pH 5.0) had a 5 $\mu\text{g ml}^{-1}$ final concentration.

Monoclonal 3E5 was purified from ascitic fluid (kindly supplied by Dr Emiliana Brocchi, IZSLE, Brescia, Italy) using a HiTrap Protein A affinity column (Pharmacia Biotech) and quantitated spectrophotometrically [1 OD₂₈₀ = 0.75 mg ml⁻¹]. The mAb was concentrated by precipitation in 45% (NH₄)₂SO₄, resuspension and dialysis in PBS to give 3 mg mAb in 2 ml PBS. To obtain the Fab fragment, this solution was incubated at 37°C for 5 h with 30 μg of papain (Sigma), 24 μl of 100 mM EDTA and 126 μl of 100 mM cysteine in a total volume of 3 ml PBS. Digestion was quenched with iodoacetamide (180 μl) and proteins were precipitated by 85% (NH₄)₂SO₄ and centrifugation at 10000 rpm for 20 min; the pellet was re-suspended in the minimum volume of 1:1 PBS:buffer A and dialyzed overnight against buffer A (112.4 g l⁻¹ glycine, 175.4 g l⁻¹ NaCl, pH 8.9). The protein solution was passed through the HiTrap Protein A column; the eluate was concentrated on Centriprep-3 (Amicon) and rechromatographed on Sephadex G-100 (PBS); Fab-containing fractions were pooled, concentrated and quantitated by optical density at 280 nm.

2.3. Surface plasmon resonance analysis

2.3.1. Direct single-step kinetic analysis on mAb surfaces

BIAcore 1000 instrument, CM5 sensor chips, HBS buffer (10 mM Hepes with 0.15 M NaCl, 3.4 mM EDTA and 0.005% surfactant P20 at pH 7.4), amine coupling kit (NHS, *N*-hydroxysuccinimide; EDC, *N*-ethyl-*N'*-dimethylaminopropylcarbodiimide) and ethanolamine were all from Biosensor AB. Immobilization of mAbs was performed according to the manufacturer's instructions, a 5 $\mu\text{l min}^{-1}$ HBS continuous flow was maintained and the carboxymethyl surface was activated by a 7-min injection of a solution containing 0.2 M EDC and 0.05 M NHS; biospecific surfaces were

obtained by injecting 35 μl of the mAb solutions; unreacted activated groups were blocked by a 6-min injection of ethanolamine and remaining non-covalently bound molecules were washed off with a 3-min pulse of 100 mM HCl for SD6 or 10 mM NaOH for 4C4 and 3E5 surfaces. Final surface densities were typically around 1500 resonance units (RU).

All kinetic SPR analyses were run at a 60 $\mu\text{l min}^{-1}$ HBS flow and each peptide was injected at six different concentrations, ranging from ca. 80–2500 nM for SD6, ca. 40–1250 nM for 4C4 and ca. 20–625 nM for 3E5 surfaces. Sensorgrams were generated by injections of peptide solutions with 90 s association steps followed by 240 s dissociation in running buffer (kinjection mode). A 90 s pulse of 100 mM HCl or 10 mM NaOH (SD6 and 4C4/3E5 surfaces, respectively) was applied to regenerate the surfaces at the end of each cycle and washing steps were added to avoid carry-over. The scrambled pentadecapeptide A15scr, injected under the same conditions, was used as a control for non-specific binding and instrumental drift effects.

Biosensor data were prepared, modeled and fitted by means of BIAevaluation 3.0.2 software [17], where calculations are carried out by numerical integration [18] and global curve fitting is done by non-linear least-squares analysis [19] applied simultaneously to the entire data set. The quality of the fitted data was evaluated by visual comparison between calculated and experimental curves, by the magnitudes of the χ^2 parameter and of the standard errors associated to the constants obtained.

2.3.2. Direct single-step kinetic analysis on peptide surfaces

SPR experiments were also run in reverse order, immobilized peptide and mAb as the soluble reactant. The immobilization procedure was identical to the one described above for mAbs, injection of 25 μl of peptide solutions (ca. 200 $\mu\text{g ml}^{-1}$ in 10 mM acetate buffer, pH 5.0) over the activated surfaces produced final immobilization responses (R_{immob}) of ca. 170 RU. mAb solutions (in HBS buffer) ranged from 25 to 800 nM (SD6) and from 16 to 500 nM (4C4 and 3E5) and sensorgrams were run, modeled and fitted as above.

2.3.3. Solution-affinity SPR analysis

Peptide–Fab interactions were studied by overnight incubation of varying peptide concentrations with a constant total Fab concentration, followed by SPR quantitation of the remaining free Fab at equilibrium. Fab–peptide mixtures in HBS were incubated overnight at 4°C, followed by 1 h re-equilibration at 25°C.

A sensor chip surface containing the wild-type peptide A15S8c1 was prepared according to the manufac-

turer's instructions, a 5 $\mu\text{l min}^{-1}$ HBS continuous flow was maintained and the carboxymethyl surface was activated by a 7-min injection of a solution containing 0.2 M EDC and 0.05 M NHS; A15S8c1 surfaces were obtained by injecting 35 μl of a 200 $\mu\text{g ml}^{-1}$ peptide solution in 10 mM sodium acetate buffer, pH 5.5. Unreacted activated groups were blocked by a 6-min injection of ethanolamine and remaining non-covalently bound molecules were washed off with a 3-min pulse of 50 mM HCl. The final immobilization response was ca. 260 RU, corresponding to a surface peptide density of ca. 0.26 ng mm^{-2} (0.26 pmol). Different solutions of Fab in HBS with known concentrations were injected over the A15S8c1 sensor chip surface in order to calculate a calibration curve. The peptide–Fab mixtures were then injected over the same surface and the amount of remaining free Fab after equilibrium was measured. All injections were run at a 5 $\mu\text{l min}^{-1}$ HBS flow and a 2-min pulse of 50 mM HCl was used to regenerate the surface at the end of each cycle. Biosensor data were fitted by means of BIAevaluation 3.0.2 software. The calibration curve *binding rate versus Fab concentration* was fitted to a four-parameter equation and then used to calculate the free Fab concentrations in the equilibrium mixtures analyzed. Free Fab dependence on peptide concentration was plotted and the affinity binding constant (K_i) was calculated using the Cheng and Prusoff's formula [20] (Eq. (1)):

$$K_i = \frac{(1 + K_A[\text{Fab}])}{\text{IC}_{50}} \quad (1)$$

where IC_{50} is the concentration of peptide competitor giving a 50% decrease in Fab concentration and K_A is the immobilized peptide — Fab affinity as measured in direct kinetic SPR analysis. This formula takes into account the influence of immobilized antigen competing with soluble antigens for the same Fab molecules.

2.4. Two-dimensional proton magnetic resonance

Spectra were acquired at 25°C, both in aqueous solution (85% $\text{H}_2\text{O} + 15\% \text{D}_2\text{O}$) and in the presence of the structuring agent TFE (30% TFE + 60% $\text{H}_2\text{O} + 10\% \text{D}_2\text{O}$) at a peptide concentration of 2 mM, with 1,4-dioxane added as an internal reference. All experiments were carried out on a Varian VXR-500 S NMR spectrometer and further processed with the VNMR software programs. The 2D $^1\text{H-NMR}$ [21] experiments performed were (i) TOCSY [22] (70 ms mixing time); (ii) NOESY [23] (200 or 400 ms mixing time); (iii) ROESY [24] (200 ms mixing time). Water signal elimination was carried out either upon pre-saturation or using the WATERGATE [25] method.

Table 2
Specificity of the anti-GH loop mAbs assayed^a

mAb	¹³⁶ YTASARGDLAHLTT ¹⁵⁰ T
SD6	—
4C4	—
3E5	—

^a The minimal location of SD6, 4C4 and 3E5 epitopes, as deduced by studies with synthetic peptides and variant viruses, is outlined by a thick line; a thinner line indicates some effect on binding of the corresponding residues. See [4] for further details.

Prior to the Fourier transform, both FIDs and interferograms were multiplied by an exponential function.

3. Results and discussion

3.1. Direct SPR analysis of small peptides

Synthetic peptides (Table 1) reproducing the GH loop of three type C FMDV variants were tested against three anti-FMDV mAbs characteristic of this antigenic site, with the specificities outlined in Table 2. In order to achieve a simple and efficient screening of the FMDV peptides, the mAbs were immobilized and the peptides were used as soluble analytes. As we have shown earlier, despite the fairly small size (ca. 1.6 kDa) of the peptides, reliable data can be obtained with this analysis configuration [10,11]. All the measurable interactions fitted to the pseudo-first-order

Table 3
Affinity data for the interactions between mAbs SD6, 4C4 and 3E5, and peptides from the G–H loops of FMDV C-S8c1, C₁-Brescia and C-S30

mAb	Peptide	$K_{A(\text{kin}1)}$ (M^{-1}) ^a	$K_{A(\text{kin}2)}$ (M^{-1}) ^a	K_i (M^{-1}) ^a
SD6	A15	5.4×10^7	5.0×10^7	6.3×10^7
	A15Brescia ^b	1.2×10^7	—	6.5×10^7
	A15S30	4.3×10^5	1.6×10^5	nm ^c
	cyc16S30	4.0×10^6	4.8×10^6	7.5×10^6
4C4	A15	1.9×10^8	1.1×10^8	2.0×10^7
	A15Brescia ^b	1.6×10^8	—	1.5×10^8
	A15S30	2.0×10^6	2.3×10^6	1.1×10^7
	cyc16S30	1.4×10^8	1.1×10^8	1.8×10^8
3E5	A15	9.4×10^7	1.7×10^8	2.0×10^8
	A15Brescia ^b	1.0×10^8	—	1.1×10^8
	A15S30	4.5×10^6	3.2×10^6	8.2×10^6
	cyc16S30	8.4×10^7	5.0×10^7	8.4×10^7

^a $K_{A(\text{kin}1)}$, affinity from SPR kinetic analysis with immobilized mAb; $K_{A(\text{kin}2)}$, affinity from SPR kinetic analysis with immobilized peptide; $K_{i(\text{sol. aff.})}$, affinity from solution affinity SPR analysis, using the Cheng and Prusoff's formula.

^b Extremely small k_d were observed using mAb as analyte.

^c nm, non-measurable under the conditions employed.

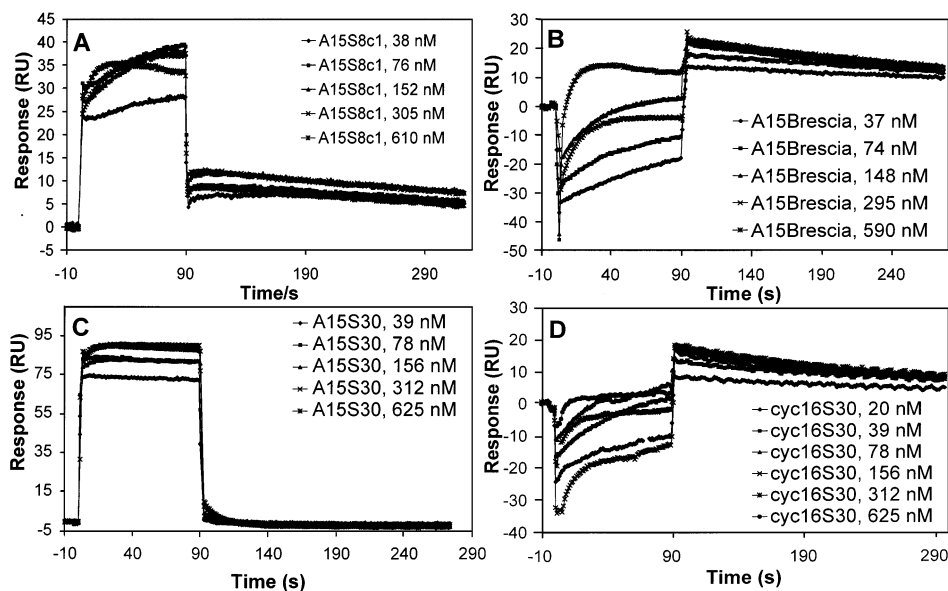


Fig. 1. Sensorgrams for the interactions between immobilized mAb 4C4 and peptides: (A) A15S8c1, (B) A15Brescia, (C) A15S30, (D) cyc16S30.

1:1 kinetic model and results were self-consistent [26]. Data (Table 3) showed that peptide A15S30 was only modestly recognized relative to peptides A15S8c1 and A15Brescia, with major differences observed in the dissociation rate constants (Fig. 1). However, the cyclic disulfide version of A15S30, peptide cyc16S30, displayed affinities comparable to those of the C-S8c1 and C₁-Brescia antigens (Table 3).

3.2. Direct SPR analysis with mAbs as analytes

Choosing peptide immobilization and mAb as analyte has some disadvantages, (1) comparison between different peptides is often unreliable, since it is difficult to reproduce immobilization conditions; (2) too much peptide is required to obtain measurable immobilization responses, leading to problems such as ligand site heterogeneity or diffusion-controlled kinetics. Finally, (3) the large size of the mAb tends to favor steric hindrance and diffusion-controlled kinetics [27].

These problems were confirmed by the observation of smaller rate constants (though giving similar affinities), when mAb was used as analyte. This analysis configuration was used only for comparison purposes, and was not subjected to extensive optimization. A fine-tuning of peptide immobilization would be required and, further, Fab fragment instead of whole mAb should be used as analyte to ensure a 1:1 binding interaction. Anyway, results obtained in these SPR analyses were totally consistent with the SPR data obtained in the reverse configuration, confirming the affinity ranking already found for the peptides under study (Table 3). Again, major differences were observed in dissociation rate constants (Fig. 2).

3.3. Solution affinity SPR analyses

The peptide–Fab affinity in solution was also measured by means of the SPR biosensor. The goal of this experiment was two-fold, first, to confirm data derived from the SPR kinetic analyses and, second, to analyze if prolonged incubation of peptide A15S30 with the antibody would promote peptide rearrangement to a more antigenic conformation. Indeed, we confirmed that most solution affinity constants were identical to those derived from the kinetic SPR experiments. This excellent agreement had only one remarkable exception, peptide A15S30, for which significantly higher affinities towards mAbs 4C4 and 3E5 were observed in solution (Table 3, Fig. 3). This behavior of peptide A15S30 and the higher reactivity observed for peptide cyc16S30 (Table 3, Fig. 3) highlight the pertinence of introducing conformational constraints for accurate modeling of the C-S30 GH loop by synthetic peptides.

3.4. Nuclear magnetic resonance studies

In view of the results obtained in the SPR analysis of the FMDV peptides, we searched for structural elements that could account for the antigenicity rankings observed. For this purpose, we performed a 2D-¹H NMR study of peptides A15S30 and cyc16S30 both in water and in 30% TFE.

The first structural information withdrawn from the NMR experiments was based on the conformational chemical shifts. As can be seen in Fig. 4, neither peptide shows any marked tendency to adopt a predominant conformation in solution. The small absolute values of the conformational chemical shifts suggest that both

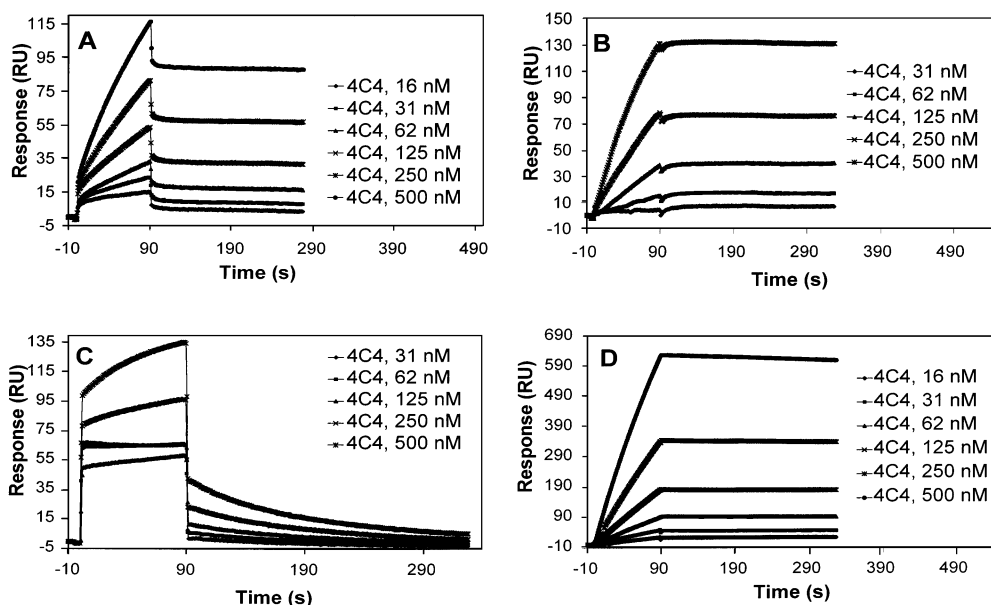


Fig. 2. Sensorgrams for the interactions between mAb 4C4 in solution and immobilized peptides: (A) A15S8c1, (B) A15Brescia, (C) A15S30, (D) cyc16S30.

peptides exist mainly in aperiodic (random coil) form in solution. This lack of structuration could not be modified by environmental changes, as shown by the similarity between conformational chemical shifts observed in water and in 30% TFE. Even so, a certain tendency to structuration in the central region of these peptides can be distinguished. As reported earlier for the linear (A15S8c1) and cyclic disulfide (AhxA16SS) versions of FMDV C-S8c1 [14,28], the conformational chemical shifts in the region that includes the RGD tripeptide are compatible with an open turn conformation. Further, the cluster of negative conformational chemical shifts from ^{143}Asp to ^{146}His could be suggestive of an incipient short helix in this region, as also reported for the C-S8c1 peptides [14,28]. A difference between the peptides of both strains is, however, the fact that this short helix extends, in the C-S8c1 peptides, to the ^{147}Leu residue. In the case of the C-S30 peptides, the replacement of leucine by valine at this position seems to shorten this pre-helical stretch, and this could be related to the lower antigenicities observed in peptides bearing this replacement. This seems further supported by the fact that absolute values of conformational chemical shifts are higher for cyclic peptide cyc16S30, which is the best of the two C-S30 antigens under study.

NOESY spectra were not particularly conclusive. A continuous series of $\alpha\text{N}_{i,i+1}$ and $\beta\text{N}_{i,i+1}$ nuclear Overhauser effects (NOEs) was observed for both peptides either in water or in 30% TFE (not shown). These NOEs are compatible with practically all conformations, and therefore, not very informative. Some weak $\text{NN}_{i,i+1}$ NOEs — compatible with α helix — were

observed for peptide A15S30 in 30% TFE, in the same region where the helical stretch had been proposed (not shown). In turn, peptide cyc16S30 displayed weak $\text{NN}_{i,i+1}$ NOEs both in water and 30% TFE (not shown). Peak assignment was often ambiguous due to identical chemical shifts for different H^{N} and peak overlap possibly prevented the detection of other informative $\text{H}^{\text{N}}-\text{H}^{\text{N}}$ connectivities.

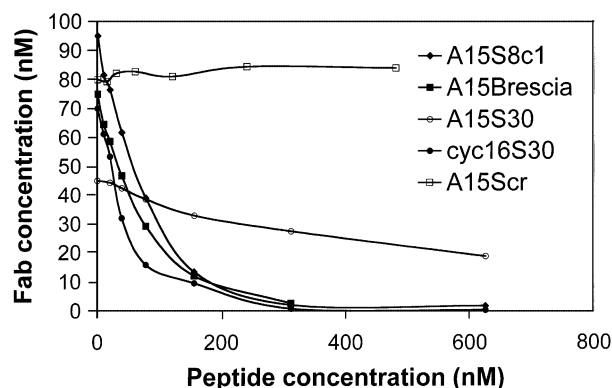


Fig. 3. Inhibition curves for peptides A15S8c1, A15Brescia, A15S30, cyc16S30 and A15Scr (negative control) in solution affinity SPR experiments. Note: varying concentrations of peptides were incubated with a constant concentration of Fab overnight and remaining free Fab was then quantitated by SPR using an A15S8c1 surface; [free Fab]_{cq} was plotted against peptide concentration to determine the corresponding IC_{50} s and thus calculate affinities (K_{D}) by means of the Cheng and Prusoff's formula (see text).

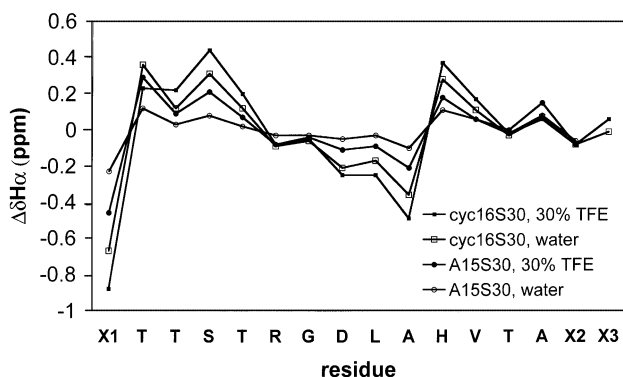


Fig. 4. Conformational chemical shift plot for peptides A15S30 (X1, Tyr; X2, Thr; X3, –) and cyc16S30 (X1, Cys; X2, Ahx; X3, Cys) in water and 30% TFE.

3.5. Relevance of conformation in linear antigenic sites

The usefulness of cyclization as a means to enhance the antigenicity of peptides that, in the linear form, do not suitably reproduce the antigenic behavior of the native antigen has been generally acknowledged [14,29–33]. In this work, we have successfully applied the cyclization approach to the GH loop of FMDV C-S30 and found an improvement of two orders of magnitude in the recognition by mAb 4C4 relative to the linear form. This finding illustrates once more the importance of a correct folding in any attempt to mimic a *continuous* antigenic site. When successfully achieved, cyclization provides the structural preorganization required to access the bioactive (antibody-binding) conformations in an energetically efficient way.

Another relevant finding of the present work is that antigenic cross-reactivity may be strongly dependent on the assay format, as shown by the comparison of our results with earlier enzyme immuno-electrotransfer blot (EITB) (using capsid protein VP1 [3]) and enzyme immunodot (EID) (using a peptide-KLH conjugate [13]) data. Similar problems have been observed earlier and discussed on the basis that the microscopic environment supporting the peptide (e.g. virus particle, viral protein, protein carrier, crystal, solution) may significantly affect its presentation and thus influence antigenic recognition [34].

4. Conclusions

Extensive research on 15-mer peptide mimics of FMDV antigenic site A has provided a solid basis for the adequacy of such peptides as models of this antigenic site. However, an exception was observed in the present work, where the linear peptide A15S30 was seen to be less antigenic than expected from earlier immunoenzymatic and crystallographic studies. In this case,

peptide conformation appeared to play a crucial role, since none of the replacements is directly involved in epitope–paratope contacts. Indeed, allowing the peptide to adopt a proper folding by prolonged incubation with antibody (solution affinity SPR) or, alternatively, inducing it into a native-like conformation by cyclization (peptide cyc16S30) led to good antigenic responses and to a higher degree of structural similarity with reference strain C-S8c1 peptides.

These findings have obvious implications for the design of synthetic peptide-based vaccines, since they reinforce the importance of peptide conformation even when continuous (i.e. linear) epitopes are to be mimicked.

Real-time biospecific interaction analysis, by means of SPR biosensors, is again shown to be rather useful in the functional analysis of antigenic determinants, allowing to detect differences in peptide antigenicity that could not be distinguished by other means, not even by structural studies of the peptide–antibody complex.

Acknowledgements

We thank Drs Wendy Ochoa, Núria Verdaguer and Ignasi Fita (IBMB — CSIC, Barcelona), for supplying mAbs SD6 and 4C4, as well as for helpful discussions. We also thank Dr Emiliana Brocchi (IZSLE, Brescia, Italy) for supplying mAb 3E5 and *Serveis Científico-Tècnics* (SCT, University of Barcelona) for supplying all the BIAcertified materials and the BIAcore 1000 instrument. PG thanks the *Fundação Calouste Gulbenkian* (Lisbon, Portugal) for her Ph.D. grant and the University of Porto (Oporto, Portugal) for a temporary leave from teaching duties. This work was supported by grants PB97-0873 and BIO99-0484 (DGICYT) and by *Generalitat de Catalunya (Grup Consolidat and Centre de Referència en Biotecnologia)*.

References

- [1] Pereira HG. Foot-and-mouth disease virus. In: Gibbs RPJ, editor. Virus diseases of food animals, vol. 2. New York: Academic Press, 1981:333–63.
- [2] Strohmaier KR, Franze R, Adam KH. Location and characterization of antigenic portion of the FMDV immunizing protein. *J Gen Virol* 1982;59:295–306.
- [3] Mateu MG, Martínez MA, Capucci L, Andreu D, Giralt E, Sobrino F, Brocchi E, Domingo E. A single amino acid substitution affects multiple overlapping epitopes in the major antigenic site of foot-and-mouth disease virus of serotype C. *J Gen Virol* 1990;71:629–37.
- [4] Hernández J, Valero ML, Andreu D, Domingo E, Mateu MG. Antibody and host cell recognition of foot-and-mouth disease virus (serotype C) cleaved at the Arg-Gly-Asp (RGD) motif: a structural interpretation. *J Gen Virol* 1996;77:257–64.

- [5] Carreño C, Roig X, Cairó J, Camarero JA, Mateu MG, Domingo E, Giralt E, Andreu D. Studies on antigenic variability of C strains of foot-and-mouth disease virus by means of synthetic peptides and monoclonal antibodies. *Int J Pept Protein Res* 1992;39:41–7.
- [6] Mateu MG, Andreu D, Domingo E. Antibodies raised in a natural host and monoclonal antibodies recognize similar antigenic features of foot-and-mouth disease virus. *Virology* 1995;210:120–7.
- [7] Valero ML, Camarero JA, Adeva A, Verdaguer N, Fita I, Mateu MG, Domingo E, Giralt E, Andreu D. Cyclic peptides as conformationally restricted models of viral antigens: application to foot-and-mouth disease virus. *Biomed Pept Protein Nucl Acids* 1995;1:133–40.
- [8] Verdaguer N, Mateu MG, Andreu D, Giralt E, Domingo E, Fita I. Structure of the major antigenic loop of foot-and-mouth disease virus complexed with a neutralizing antibody: direct involvement of the Arg-Gly-Asp in the interaction. *EMBO J* 1995;14:1690–6.
- [9] Verdaguer N, Sevilla N, Valero ML, Stuart D, Brocchi E, Andreu D, Giralt E, Domingo E, Mateu MG, Fita I. A similar pattern of interaction for different antibodies with a major antigenic site of foot-and-mouth disease virus: implications for intratypic antigenic variation. *J Virol* 1998;72:739–48.
- [10] Gomes P, Giralt E, Andreu D. Surface plasmon resonance screening of synthetic peptides mimicking the immunodominant region of C-S8c1 foot-and-mouth disease virus. *Vaccine* 2000;18:362–70.
- [11] Gomes P, Giralt E, Andreu D. Direct single-step surface plasmon resonance analysis of interactions between small peptide analytes and immobilized monoclonal antibodies. *J Immunol Methods* 2000;235:101–11.
- [12] Ochoa WF, Kalko SG, Mateu MG, Gomes P, Andreu D, Domingo E, Fita I, Verdaguer N. Structure of a multiply substituted G-H loop from foot-and-mouth disease virus in complex with a neutralizing antibody. *J Gen Virol* 2000; 81:1495–505.
- [13] Mateu MG, Andreu D, Carreño C, Roig X, Cairó J, Camarero JA, Giralt E, Domingo E. Non-additive effects of multiple amino acid substitutions on antigen-antibody recognition. *Eur J Immunol* 1992;22:1385–9.
- [14] Valero ML, Camarero JA, Haack T, Mateu MG, Domingo E, Giralt E, Andreu D. Native-like cyclic peptide models of a viral antigenic site: finding a balance between rigidity and flexibility. *J Mol Recognit* 2000;13:5–13.
- [15] Fields GB, Noble RL. 9-fluorenylmethoxycarbonyl amino acids in solid phase peptide synthesis. *Int J Pept Protein Res* 1990;35:161–214.
- [16] Lloyd-Williams P, Albericio F, Giralt E. Chemical approaches to the synthesis of peptides and proteins. Boca Raton: CRC Press, 1997.
- [17] BIAevaluation 3.0 software handbook. Uppsala: Biosensor AB, 1997.
- [18] Morton TA, Myszka DG, Chaiken IM. Interpreting complex binding kinetics from optical biosensors: a comparison of analysis by linearization, the integrated rate equation and numerical integration. *Anal Biochem* 1995;227:176–85.
- [19] O'Shannessy DJ, Brigham-Burke M, Soneson KK, Hensley P, Brookes I. Determination of rate and equilibrium constants for macromolecular interactions using SPR: use of non-linear least squares analysis methods. *Anal Biochem* 1993;212:457–68.
- [20] Lazareno S, Birdsall NJ. Estimation of competitive antagonist affinity from functional inhibition curves using the Gaddum, Schild and Cheng-Prusoff equations. *Br J Pharmacol* 1993;109:1110–9.
- [21] Wüthrich K. NMR of proteins and nucleic acids. New York: Wiley, 1986.
- [22] Braunschweiler L, Ernst RR. *J Magn Reson* 1983;53:521.
- [23] Kumar A, Ernst RR, Wüthrich K. *Biochem Biophys Chem Commun* 1980;95:1.
- [24] Bothner-By AA, Stephens RL, Lee J, Warren CD, Jeanloz RW. Structure determination of a tetrasaccharide: transient nuclear Overhauser effects in the rotating frame. *J Am Chem Soc* 1984;106:811–3.
- [25] Piotto M, Saudek V, Sklenár VJ. *Biomol NMR* 1992;2:661–5.
- [26] Schuck P, Minton AP. Kinetic analysis of biosensor data: elementary tests for auto-consistency. *Trends Biochem Sci* 1996;21:458–60.
- [27] Schuck P. Reliable determination of binding affinity and kinetics using surface plasmon resonance biosensors. *Curr Opin Biotech* 1997;8:498–502.
- [28] Haack T, Camarero JA, Roig X, Mateu MG, Domingo E, Andreu D, Giralt E. A cyclic disulfide peptide reproduces in solution the main structural features of a native antigenic site of foot-and-mouth disease virus. *Int J Biol Macromol* 1997;20:209–19.
- [29] Joisson C, Kuster F, Plaué S, Van Regenmortel MHV. Antigenic analysis of bean pod mottle virus using linear and cyclized synthetic peptides. *Arch Virol* 1993;128:299–317.
- [30] Müller S, Plaué S, Samama JP, Vallete M, Briand JP, Van Regenmortel MHV. Antigenic properties and protective capacity of a cyclic peptide corresponding to site A of influenza virus haemagglutinin. *Vaccine* 1990;8:308–14.
- [31] Richalet-Secordel PM, Zeder-Lutz G, Plaué S, Sommermeyer-Leroux G, Van Regenmortel MHV. Cross-reactivity of monoclonal antibodies to a chimeric V3 peptide of HIV-1 with peptide analogues studied by biosensor technique and ELISA. *J Immunol Methods* 1994;176:221–34.
- [32] Richalet-Secordel PM, Deslandres A, Plaué S, You B, Barré-Sinoussi, Van Regenmortel MHV. Cross-reactive potential of rabbit antibodies raised against a cyclic peptide representing a chimeric V3 loop of HIV-1 gp120 studied by biosensor technique and ELISA. *FEMS Immunol Med Microbiol* 1994;9:77–88.
- [33] Van der Werf S, Briand JP, Plaué S, Bourckard G, Girard M, Van Regenmortel MHV. Ability of linear and cyclic peptides of neutralization antigenic site 1 of poliovirus type 1 to induce virus cross-reactive and neutralizing antibodies. *Res Virol* 1994;145:349–59.
- [34] Van Regenmortel MHV. Structure of viral B-cell epitopes. *Res Microbiol* 1990;141:747–56.